

Implementation of the Unified Algorithm for RICH

Denis Dujmić

July 25, 2001

1 Introduction

The *Unified Algorithm for RICH* is described in [1], and marks a direction in the analysis that uses the Čerenkov counter as both a tracking and a particle identification device.

In the traditional approach, a seed track provides the ring center, and the fitting of ring signal and background photons is the preferred way of dealing with the particle identification (e.g. [2]). This school has produced two algorithms for the HERA-B RICH: RIRE [3], [4] and RITER [5] that also makes a global fit.

Beside the high occupancy due to electron showers, the particle identification is plagued with errors in the track direction - these error are consequences of the unfinished commissioning, and the design limitations of the tracking detector. It is widely believed that the angular resolution of the RICH detector ($\sim 1/3$ mrad in tx , ty) exceeds the precision of the tracker seeds (~ 0.5 mrad in tx , and ~ 1.0 mrad in ty). Therefore, it must be advantageous to include the fitting of the ring center in the evaluation of the particle identification probability.

The particle identification is done in three distinct momentum regions: *(i)* below the radiation threshold, *(ii)* low photon yield region where the ring fit is not possible, *(iii)* high photon yield region where both the ring fit and the likelihood evaluation are possible. This report deals with the evaluation of the ring parameters and the selection of the most likely hypothesis.

2 Implementation

The code uses standard tools for the photon direction reconstruction [6], the fitting formalism outlined in [1], and some routines from stand-alone Ringsearch program (RISE) [7].

The seeds are provided from RTRA¹ table taking only tracks that have hits in the VDS and tracking detectors.

In the first step, each track is assigned five hypothetical rings (e, μ, π, K, p) and five sets of photons that fall inside the range of interest (ROI) of each ring.

Below-the-threshold hypotheses

Hypotheses that are below the radiation threshold are marked as such, and omitted from further fits. Although their probabilities are set to the lowest value, they can still be taken into consideration if all above-the-threshold hypotheses fail to give a reliable ring parameters which is possible if the seed track comes from a heavy, non-radiating particle. However, it is also possible that the seed belongs to a ghost track which can depend on the tracking algorithm, interaction rate, and trigger conditions.

Additional twist to the kaon identification comes from the geometrical acceptance of pions that starts dropping for momenta below the kaon threshold, 10 GeV/c (Fig. 1). This further complicates the identification as out-of-acceptance pion can be identified as below-the-threshold kaons.

Therefore, it is left up to a user to decide how clean are the seed tracks, and how reliable is the below-the-threshold hypothesis. It is a question that can be best answered with a particular reconstruction goal in mind.

Low photon yield hypotheses

Hypotheses for which we expect a low number of photons, either because of the proximity to the radiation threshold or the shadowing of the photons, are hard or impossible to fit. If the number of photons in ROI falls below the fitting threshold, the ring is not fitted but the likelihood ($\mathcal{L}/\mathcal{L}_B$ defined with Eq. (18) in [1]) of the ring is calculated. The fitting threshold is adjustable by the user and is set to the lowest possible value (four) by default.

¹probably Random TRack Approximation

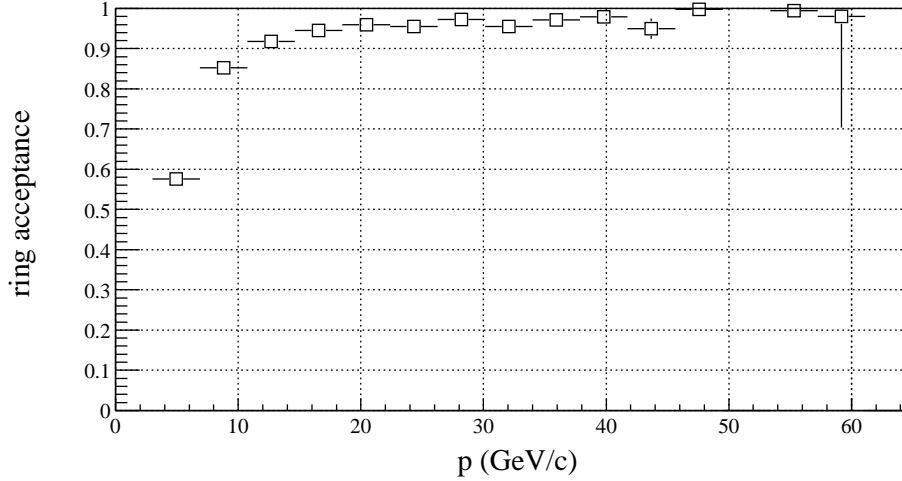


Figure 1: Ring acceptance for pions.

High photon yield hypotheses

Hypotheses with enough photons in ROI are fitted for the best ring parameters (ring center and radius). The fitting of the parameters can be switched on or off in order to make the fitting procedure more flexible (e.g. in the fitting of the medium size rings, it may be prudent to fit the ring center only and keep the radius fixed at the hypothetical value).

A fitting problem occurred in the test reconstruction that was due to the underestimate of the covariance matrix of the seed - for that reason two scaling factors are introduced for adjusting the errors in the seed direction.

Monte carlo studies showed stability of the fitting procedure with angular resolution better than 0.3 mrad for both tx and ty . The number of iterations is between 5 and 15 for the initial fit, and less than 5 for the subsequent global fit. In the available data set, the maximum average time per event was for a single muon trigger (1/3 sec).

Choice of the best hypothesis

In most of cases, we have to choose between hypotheses that have ring parameters fitted, and those that have parameters fixed at hypothetical values.

If the fit systematically underestimates the number of signal photons

S (or overestimates the number of expected photons) the likelihood may favor heavier hypotheses with lower expectation on the number of photons. Therefore, the photon yield term in the likelihood is modified

$$\mathcal{N}_0 \mathcal{T} f_s^2 r_h^2 - S \rightarrow \mathcal{N}_0 \mathcal{T} f_s^2 r_h^2 Y - S \quad (1)$$

where $\mathcal{N}_0 \mathcal{T} \approx 11,500$, f_s is the shadowing factor, r_h is the hypothetical ring radius, and Y is the yield tuning factor. The reason for the photon underestimate is not fully understood, initial tests suggested Y of about 0.8 which was then taken as default.

Another bias can come from the χ^2 term in the likelihood that gives the deviation of the ring parameters from the seed direction and the expected radius size. When rings are not fitted, this term is always zero, while for fitted rings it is in general positive. In order to prevent a penalty for improving the ring parameters, this term is omitted from the likelihood calculation².

The best results are achieved if the selection of the most likely hypothesis is based on the highest $\mathcal{L}/\mathcal{L}_B$ ratio, and this is set as the default option in the code. During the initial fitting of ring hypotheses, the radius is fixed to the hypothetical value.

Other selection criteria are based on the deviation of the fitted radius from the hypothetical radius, or the distance from the $R2P2$ line (problem occurs when the number of ROI photons is too low and the ring cannot be fitted). There are some ongoing attempts to make a combination between the likelihood-based and ring parameter-based selections.

Representation of the result

In the first step, the main objective is to find the most likely hypothesis for each track.

This allows us to perform a global ring fit that takes into account sharing of the photons between rings. In this step all three ring parameters are fitted which gives a unique Čerenkov angle for each of the seed tracks. Using this angle, tracks are assigned five probabilities (e, μ, \dots, p) which are based on distances from the $R2P2$ lines (Eq. (38) in [1]), or deviations of the fitted radius from hypothetical radii.

Finally, in order to simplify the analysis for the user, the probabilities (e, μ, \dots, p) are normalized to one.

²it was originally introduced to contribute to the stability of the fit

3 Performance evaluation

Pion, kaon identification efficiency

The performance evaluation is based on a simple pion-kaon separation criterion³: $\mathcal{L}_\pi > \mathcal{L}_K$ for pions, and $\mathcal{L}_K > \mathcal{L}_\pi$ for kaons. The identification efficiency for pions is defined as the number of pions that satisfy this cut over the total number of pions

$$\epsilon_\pi = \frac{N_{\pi \rightarrow \pi}}{N_{\text{all } \pi}} \quad (2)$$

and, the kaon fake rate is the number of kaons identified as pions

$$\eta_{K \rightarrow \pi} = \frac{N_{K \rightarrow \pi}}{N_{\text{all } K}} \quad (3)$$

The same efficiency for kaons is

$$\epsilon_K = \frac{N_{K \rightarrow K}}{N_{\text{all } K}} \quad (4)$$

and, the pion fake rate is

$$\eta_{\pi \rightarrow K} = \frac{N_{\pi \rightarrow K}}{N_{\text{all } \pi}} \quad (5)$$

The performance convention requires that the efficiency be evaluated with the corresponding fake rate less than 5%. This rule is meaningful in case of kaons since there are roughly eight times less kaons than pions, and one wants to keep the pion leakage into kaons as small as possible. However, requiring less than 5% of kaon fake rate when evaluating the pion efficiency is only for the sake of the convention.

The efficiency is calculated using monte carlo truth to obtain the sample of pure pions and kaons. In real data, a clean source of pions is obtained from K_S signal which allows us to estimate the pion efficiency (Eq. (2)) and the pion fake rate (Eq. (5)). Figures 2 and 3 show the identification rates for the simulation and the data.

³one can easily imagine a more sophisticated identification rule

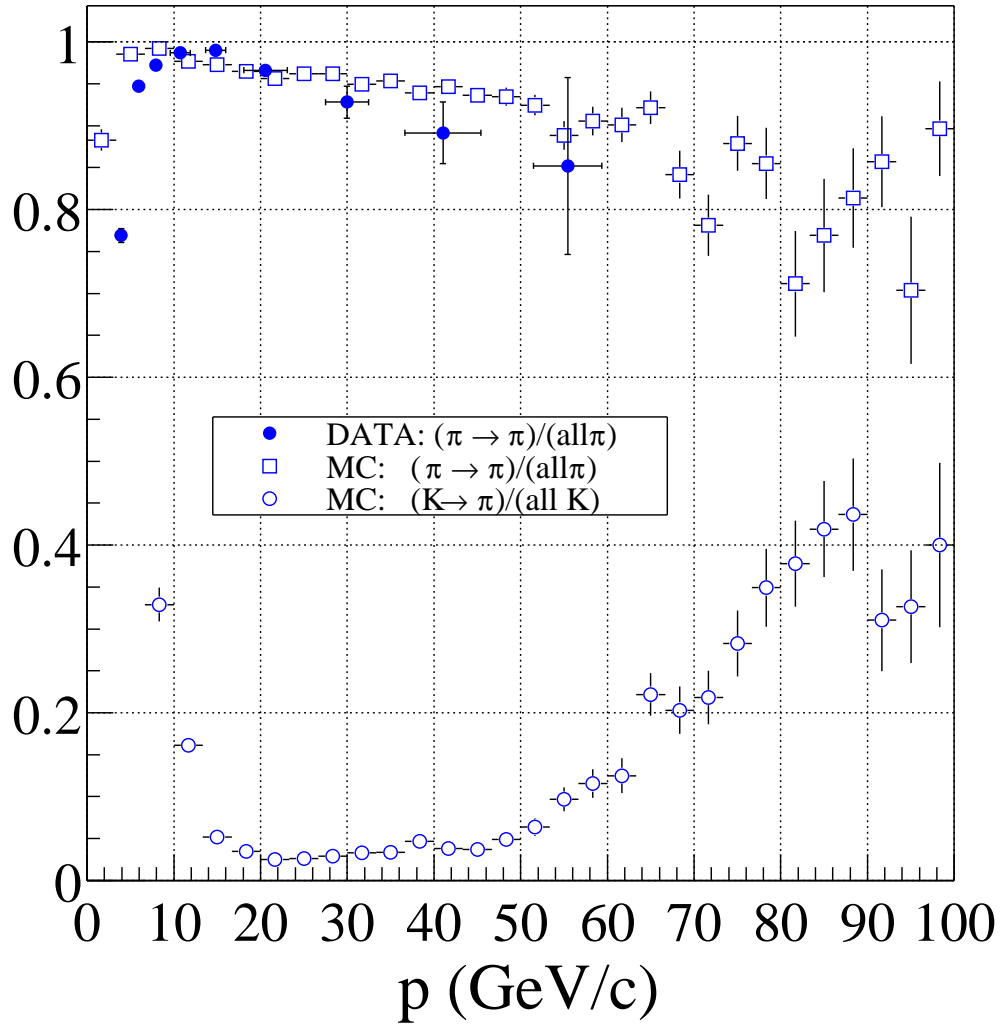


Figure 2: Pion efficiency and kaon fake rate.

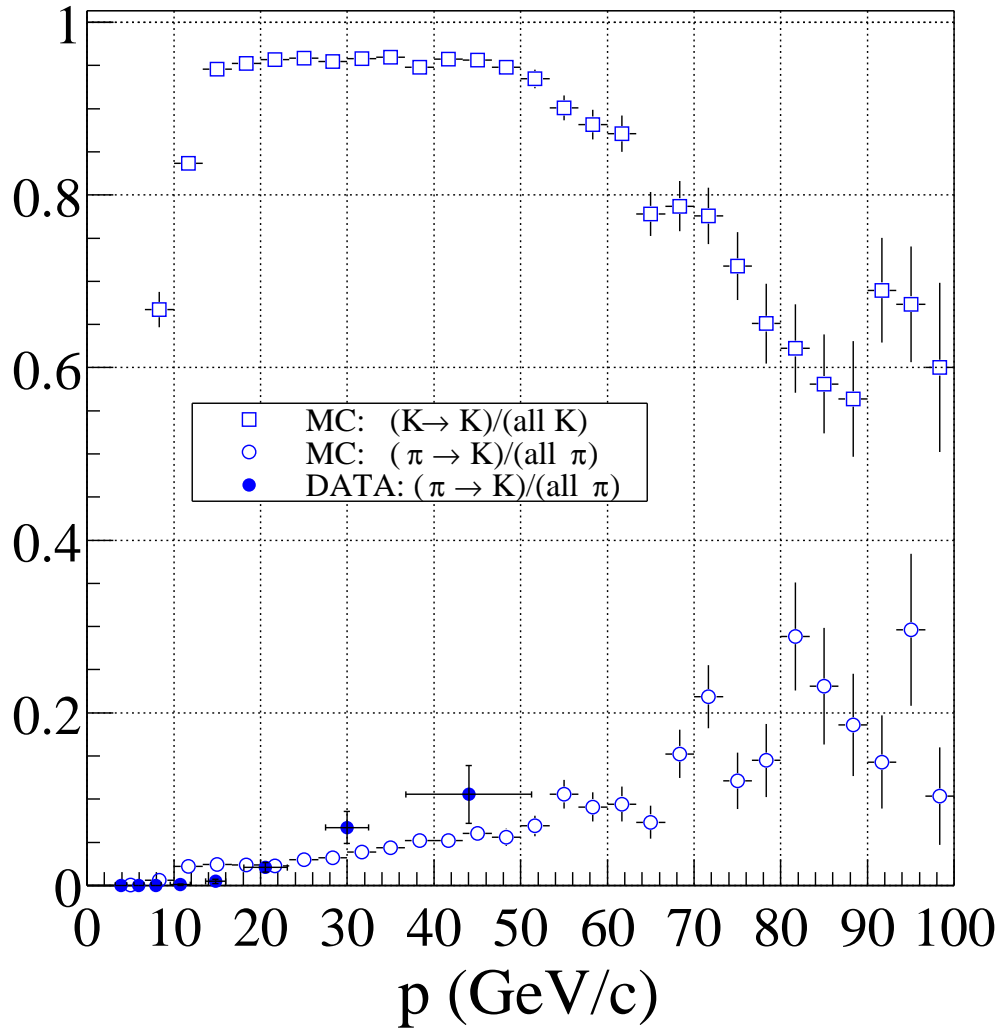


Figure 3: Kaon efficiency and pion fake rate.

Pion, kaon separation point

The separation point is defined as

$$\frac{m_K^2 - m_\pi^2}{p^2} = 2 \Sigma_\pi + 2 \Sigma_K \quad (6)$$

where Σ is the width of R2P2 bands. When the best hypothesis is chosen as the closes distance to the *R2P2* lines, the separation point occurs at $p = 57$ GeV/c. This type of hypothesis selection has a disadvantage that it cannot be applied to rings with low photon yield.

In the currently used scheme that bases the selection on the best likelihood, the pion-kaon separation point is at 48 GeV/c.

4 Summary

A new particle identification algorithm is available in the HERA-B reconstruction environment (ARTE). It uses seeds from the tracking detector, and a new likelihood approach for the fitting of RICH rings [1]. A monte carlo study shows the efficiency plateau for both pions and kaons above 90%, and the fake rates below 5% in the most of the momentum range. Pions from K_S sample in real data were used to confirm the high pion efficiency and the low pion fake rate into kaons.

Further improvements could come from a more sophisticated hypothesis selection criterion that would combine the ring likelihood and the ring parameters, and a better understanding of the systematic effects.

A ARTE output tables

RSEG	
field	saved value
xf	ϕ
yf	λ
zf	$\mathcal{L}/\mathcal{L}_B$
txf	tx
tyf	ty
time	θ
dtim	mass of best hypothesis
chi	χ^2
cmp	RICH component id
fit	12 for seeded rings, 13 for conversions
xe	D_h , R2P2 distance
ye	R_B
ze	signal photons
txe	photon acceptance
nhit	number of hits in ROI
npar	3
err	number of iterations

RTRA	
field	saved value
txr	tx
tyr	ty
flr	$e + 10 \cdot \mu + 100 \cdot \pi + 1000 \cdot K + 10000 \cdot p$ where e, \dots, p are 0 = below radiation threshold 1 = rejected 2 = possible 3 = accepted
cer	radius
lre ... lrp	likelihoods
crich	0=seeded rings > 0 for stand-alone rings

B ARTE kumac commands

Command:

RISE/RING [VERBOSE DRAD NORM PTYPE PTYPEG GLOBAL FITR
FITX FITY MAXITER SMEARX SMEARY MAXR MINL OKL MINROI TRACK
TUNEYIELD ENHTX ENHTY]

Description: Set Ring fitting parameters.

Parameters:

command	argument type	description	default value
VERB*OSE	I	Verbosity level: 0=off	0
DR*AD	R	ROI size	0.007
NORM	I	Normalize likelihoods	yes
PTYPE	I	Choose method to fill probabilities 0= θ , 1= $R2P2$, 2= $\mathcal{L}/\mathcal{L}_B$, 3= χ^2	2
PTYPEG	I	Choose method to fill probabilities in global fit: 0= θ , 1= $R2P2$	1
GL*OBAL	I	Make global fit	yes
FITR	I	Fit radius	yes
FITX	I	Fit horizontal angle	yes
FITY	I	Fit vertical angle	yes
MAXIT*ER	I	Maximum number of iterations	15
SMEARX	R	Tx track smearing in MC	0
SMEARY	R	Ty track smearing in MC	0
MAXR	R	Maximum fitting radius	0.06
MINL	R	Minimum likelihood for accepting ring	-2.5
OKL	R	Minimum likelihood for positive ID	4.5
MINROI	I	Minimum hits in ROI	4
TRACK	I	Track selection: 0=unique VDS+tracker, 1=VDS+tracker hits required	0
TUNE*YIELD	R	Set systematic error for ring yield	0.8
ENHTX	R	Seed sigma tx enhancement factor squared	20
ENHTY	R	Seed sigma ty enhancement factor squared	10

Command:
RISE/MESS*AGES

Description: Print all error messages collected during the reconstruction.

References

- [1] R. F. Schwitters, *Unified Approach to Particle Identification Using the HERA0B RICH*, **HERA-B 01-066 RICH 01-017**
- [2] P. Baillon, *Nucl. Instrum. Meth. A* **238**, 341 (1985)
- [3] T. Oest et al., *A Study of a RICH Photon Detector Design*, **HERA-B 96-190 RICH 96-023**
- [4] I. Arinyo, L. Garrido, *Particle Identification of the HERA-B RICH*, **HERA-N 99-108 RICH 99-009**
- [5] M. Starič and P. Križan, *Čerenkov Angle Reconstruction in the HERA-B RICH*, **HERA-B 95-132 RICH 95-015**
- [6] D. Dujmić, R. Eckmann, R. Schwitters, *Reconstruction of Photon Directions in the HERA-B RICH*, **HERA-B 00-019 RICH 00-005**
- [7] R. Eckmann and D. Dujmić, *Software for Stand-alone RICH Reconstruction*, **HERA-B 00-004 RICH 00-002**